Properties of LiF and Al_2O_3 to 240 GPa for Metal Shock Temperature Measurements

Kathleen G. Holland and Thomas J. Ahrens

Lindhurst Laboratory of Experimental Geophysics,
Seismological Laboratory,
California Institute of Technology, Pasadena, California

Shock temperature experiments employing a six-channel pyrometer were conducted on 200, 500, and 1000 Å thick films of Fe sandwiched between 3-mm-thick anvils of Al_2O_3 and LiF to measure the thermal diffusivity ratios Al_2O_3/Fe and LiF/Fe at high temperatures and pressures. Temperature decays of 3000 ± 800 K in 250 ns were observed at Fe pressures of 194 – 303 GPa, which reflect the conduction of heat from the thin metal films into the anvil material. These results were achieved via experiments employing LiF anvils at conditions of 164 – 165 GPa and 4190 – 4220 K and Al_2O_3 anvils at conditions of 156 – 304 GPa and 1290 – 2740 K. Thermal modeling of interface temperature versus time yields best fit thermal diffusivity ratios of 4 – 19 ± 1 (Fe/anvil) over the pressure and temperature range of the experiments. Calculated thermal conductivities for Fe, using electron gas theory, of 111 – 181 W/mK are used to calculate thermal conductivities for the anvil materials ranging from 2 to 13 W/mK. Debye theory predicts higher values of 8 to 35 W/mK. Data from previous experiments on thick ($\geq$ 100μm) films of Fe and stainless steel are combined with our present results from experiments on thin ($\leq$ 1000 Å) films to infer a 5860 ± 390 K Hugoniot temperature for the onset of melting of iron at 243 GPa. Our results address the question of whether radiation observed in shock temperature experiments on metals originates from the metal at the metal/anvil interface or from the shocked anvil. We conclude that the photon flux from the shocked assemblies recorded in all experiments originates from the metal. Within the uncertainties of the shock temperature data, the uncertainties in shock temperatures resulting from the radiation from the anvils is negligible. This is in direct disagreement with the conclusions of previous work by Kondo.

INTRODUCTION

The phase diagram and thermal properties of iron at ultra-high pressures are important because they provide vital information for understanding the Earth's core, and also because they add to the fundamental understanding of the behavior of materials at high pressure. However, experimental determination of these properties are difficult. Dynamic and static experiments each have their own challenges [*Gallagher et al.*, 1994; *Boehler*, 1994; *Williams et al.*, 1987; *Yoo et al.*, 1993] and the results in the 50 – 200 GPa range are disparate. Not only does the extrapolation of static results to higher pressure disagree with the higher pressure dynamic results, but static experiments conducted at dif-

Properties of Earth and Planetary Materials
at High Pressure and Temperature
Geophysical Monograph 101

ferent laboratories do not agree with each other. Shock temperature determinations on opaque materials such as iron are difficult because one cannot directly observe the interior of the shocked material and it is necessary to employ transparent anvil materials and observe the metal/anvil interface. This method has inherent difficulties [*Nellis et al.*, 1990], the three most important of which are addressed here. First, the shock-compressed anvil materials may have a sufficiently high opacity that they may be emitting enough light so that they interfere with the observation of the iron/anvil interface. Second, the data reduction requires knowledge of thermal parameters that are not easily measured at the conditions of the experiment. Third, imperfections at the iron-anvil interface can lead to local deposition of irreversible work and hence induce anomalously high temperatures.

When a shock wave propagates from one material to another that is both in ideal contact and has a similar shock impedance, most of the energy of a shock wave is transmitted, rather than reflected. The optical properties of Al_2O_3, which has a similar shock impedance to iron and is used as an anvil material in shock temperature experiments of metals, have been controversial. Initially *Grover and Urtiew* [1974] inferred that Al_2O_3 became opaque above 85 GPa. However both *Ahrens et al.* [1990] and *McQueen and Isaak* [1990] concluded that the Grover and Urtiew analysis was too simplified. A more detailed analysis demonstrated the transparency of Al_2O_3 to 200 GPa. *Ahrens et al.* [1990] and *Williams et al.* [1987] assumed that Al_2O_3 remained transparent while in the shocked state, implying that the anvil material is indeed a window material and that one can observe optical radiation from the metal at the anvil/metal interface. *Kondo* [1994] inferred that Al_2O_3 becomes opaque under shock loading and that observed radiation in shock temperature experiments originates from the anvil, not the metal. Thus *Kondo* claimed that shock temperature experiments on a metals may, in fact, be measuring the temperature of the anvil rather than the metal. How radiation from the metal can be distinguished from anvil radiation during a shock temperature experiment is germane, especially in view of the above results by *Kondo* [1994] with Ag films deposited on Al_2O_3. In the present paper we address this issue by studying the systematic differences in the radiation observed from sample assemblies, between experiments. For example, if observed interface temperature varies systematically with the type of metal sample used but not with the type of anvil, then the optical radiation is inferred to originate from the metal/anvil interface and therefore to reflect the properties of the metal.

One of the critical parameters that is used to calculate Hugoniot temperature from interface temperature is the thermal diffusivity ratio between the metal and the anvil, R. A series of experiments (discussed in the section on 'thin films') is carried out to measure this parameter. However, the 'thin film' experiments do not provide accurate shock temperature data for iron, so results from other experiments (discussed in the 'thick film' section) are analyzed using R values determined in 'thin film' experiments. Revised Hugoniot temperatures are reported. These results do not by themselves yield a pressure where the iron Hugoniot intersects the solid-liquid phase boundary. However, *Brown and McQueen* [1986] observed the onset of melting at 243 ± 3 GPa along the principal Hugoniot of iron by observing a decrease in sound velocity, so we have interpolated our temperatures results to infer melting at 5860 ± 390 K and 243 GPa.

In the present paper we use the lack of correlation of shock temperature with anvil material to address the issue of the origin of the optical radiation during shock temperature experiments on iron. We then discuss the data reduction of these experiments and later experiments to determine R. We also discuss issues related to effects and problems at the iron/anvil interfaces. Finally, we determine a revised phase diagram for iron, which infers a temperature for the onset of melting of an assumed ϵ phase along the principal Hugoniot.

RELEVANT EQUATIONS

Experimental observation of the temperatures of shocked metals is difficult because they are opaque. Thus, an anvil is used, and the temperature of the interface between the anvil and the metal T_i is observed. In the present case we assume the anvil has a slightly lower shock impedance than the metal sample [*Ahrens*, 1987]. We drive a shock wave into the sample inducing a Hugoniot pressure P_h, volume V_h, and temperature T_h. Upon reflection at the anvil, a release wave is reflected back into sample, resulting in a release-pressure P_r and release-density ρ_r in the metal. The temperature of the interior of the released sample [*Grover and Urtiew*, 1974] T_r is calculated from T_i via

$$T_i = T_r - \frac{T_r - T_a}{1+\alpha} \tag{1}$$

where T_a is the internal shock temperature of the anvil, and α is defined by

$$\alpha = \sqrt{\frac{k_m \rho_m C_{p_m}}{k_a \rho_a C_{p_a}}} \tag{2}$$

where $C_p = C_v(1 + \gamma\alpha^{th}T)$ is the specific heat at constant pressure, ρ is the high-pressure density, k is the thermal conductivity, α^{th} is the coefficient of thermal expansion [*Duffy*, 1993], and $C_v = 3R_u/w$ is the specific heat at constant volume, where $R_u = 8.31441$ J/K·mol is the universal gas constant, and w is the mean atomic weight. The subscript 'a' denotes the anvil material and the subscript 'm' denotes the metal. Previous authors [*Ahrens et al.*, 1990] have used C_v instead of C_p in Equation 2 and this makes only a 0.4% difference in the resulting value for α. Bass also calculated k_a from

$$k_{T,0} = A + B/T \tag{3}$$

$$k_a = k_{T,P} = k_{T,0}\left(\frac{\rho_P}{\rho_0}\right)^{2\gamma+5/3} \tag{4}$$

where $A_{Al_2O_3} = -2.599$ W/mK, $B_{Al_2O_3} = 1.176 \times 10^4$ W/m, $A_{LiF} = -0.2$ W/mK, and $B_{LiF} = 3.7 \times 10^3$ W/m are measured at ambient pressure and high temperature and γ, ρ_0, and ρ_P are the Grüneisen parameter and the initial and compressed densities of the material. Other formulations [*Leibfried and Schlömann*, 1954; *Tang*, 1994] calculate $k_{T,0}$ analytically and produce similar results in the temperature range of interest. Equation 2 assumes $\gamma = \gamma_0$; without this assumption, a lower value of k_a would be predicted. However, we use the above formulation to facilitate a direct comparison of our T_h values with the results of Bass. Fourier conduction of heat from a high temperature metal film into a lower temperature anvil material is dependent upon the thermal diffusivity ratio, R.

$$R = \frac{\kappa_m}{\kappa_a} \tag{5}$$

where κ_m and κ_a are the thermal diffusivities of the metal and the anvil material respectively. Thermal diffusivity, κ, is related to thermal conductivity, k, via

$$\kappa = k/\rho C_p \tag{6}$$

where C_p is the specific heat at constant pressure and ρ is the high pressure density. The thermal conductivity of the metal, k_m, is calculated from the Wiedemann-Franz law:

$$k_m = L\sigma T \tag{7}$$

where $L = 2.45 \times 10^{-8}$ W·Ω/K^2 is the Lorenz number, σ is the electrical conductivity of the metal, and T the is temperature. This formulation assumes that the metal acts as a free-electron gas, and that phonon effects are negligible. This assumption is supported by the k_m(Fe) data of *Secco and Schloessin* [1989]. *Manga and Jeanloz* [1996] compared Secco's data to the σ(Fe) data of *Matassov* [1977] and concluded that the Wiedemann-Franz law was valid for Fe. Note that σ has a $1/T$ dependence and also a pressure P dependence, making Equation 7 more properly $k_m(P) = L\sigma(P, 1/T)T$. Thus when calculating k_m for a thin film experiment that has a different shock temperature than the Hugoniot temperature of Fe, one must use a calculated Hugoniot temperature in Equation 7 because that is the temperature at which the measurement of σ was made [*Manga and Jeanloz*, 1997].

To determine a Hugoniot temperature for an experiment employing a 'thick film' (≥ 1 μm) an R value is used to calculate k_m/k_a via Equation 5 and Equation 6. k_m/k_a is then used to calculate α via Equation 2, and α is used to calculate T_r via Equation 1. T_h is calculated from T_r via

$$T_h = T_r \exp\left[\gamma_o\rho_o\frac{(u_r - u_h)^2}{P_h - P_r}\right] \tag{8}$$

where u_r and u_h are the released and Hugoniot particle velocities.

Equation 1 does not apply for 'thin films', where the films cannot be approximated by an infinite half-space, so to determine a Hugoniot temperature for an experiment employing a 'thin film' (≤ 1000 Å), T_r is obtained by fitting the measured T_i and the calculated T_a to a finite element model [*Gallagher and Ahrens*, 1996] for symmetric heat flow from a thin film; Equation 8 is used to calculate T_h from T_r.

SHOCK TEMPERATURE EXPERIMENTS ON METALS

The shock temperature experiments on metals were performed on a 2-stage light-gas gun [*Ahrens*, 1987] via optical pyrometry [*Yang*, 1996]. There are two different types of sample configurations used, the 'thick film' setup, using 1 μm or thicker films and the 'thin film' experiments using 200, 500, or 1000 Å films. In both cases, the metal film is in contact with the anvil materials that serve to compress the metal at high pressure. The Al_2O_3 used for our experiments was obtained from the Adolph Mueller Company as spectral grade sapphire, and the LiF was obtained from Bicron Inc. as optical grade windows. The metal surface is intended to be viewed through one of the transparent anvils during the time the shock wave passes through the anvil.

To address the issue of interface quality, we grew films of 99.995% purity iron epitaxially on our anvil materials using argon ion sputtering in ultra high vacuum 5×10^{-9} torr. The 1000 Å film that was used for Shot #287 was deposited in 40 minutes on a 500°C preheated

LiF substrate, and a shallow angled electron scattering pattern (RHEED) was observed to show that the deposited film displayed limited long-range order [*Hashim et al.*, 1993]. An SEM (Figure 1) image was obtained to demonstrate that there was no micron scale porosity. The image shows no dark patches in the uppermost light grey area, which would imply that there was measurable porosity. Additionally the image shows clearly that the length-scale of surface roughness of the anvil is much larger than the thickness of the metal film, which is the thin pale line in the center of the figure. This leads to an effective porosity in the film, which results in 'thin films' having anomalously high shock temperatures.

Thick Film Experiments

Many shock temperature experiments on metals [*Williams et al.*, 1987; *Ahrens et al.*, 1990; *Yoo et al.*, 1993] have employed thick films or foils. In these cases

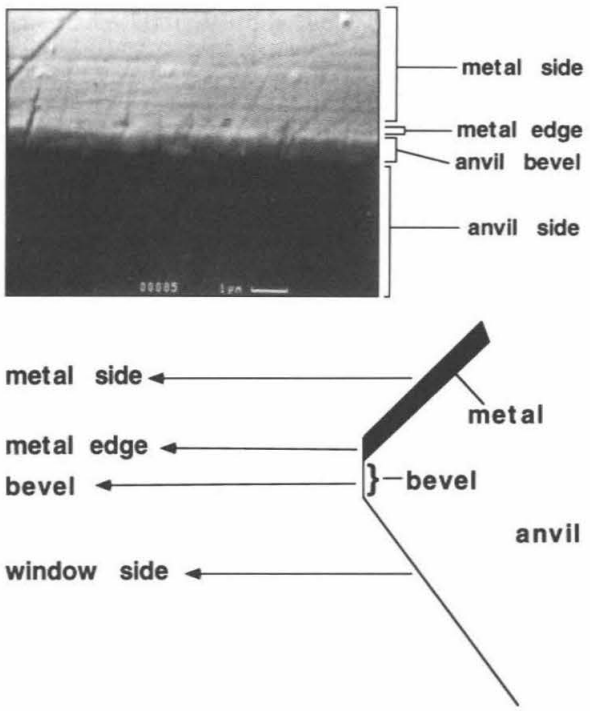

Figure 1. Scanning electron microscope image of the 1000 Å film used in Shot #297. The film is shown as deposited upon the Al_2O_3 anvil, tilted at a 45° angle to the camera. The dark lower section is the anvil, and the lighter section in the middle is the bevel at the edge of the anvil. The very thin pale line above the bevel is the edge of the Fe film, and the darker section at the top is the face of the Fe film, with the Al_2O_3 visible through the Fe.

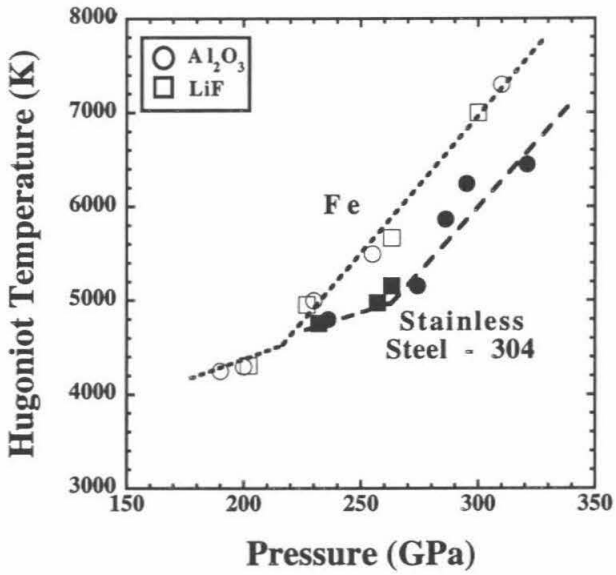

Figure 2. Comparison of Hugoniot temperatures for Fe (open symbols) and stainless steel, SS (solid symbols). Note the absence of coherent difference between temperatures for LiF (circles) and Al_2O_3 (squares).

the metal/anvil interface can be modeled as in infinite half-space. Specifically, a 'thick film' is one where the thickness is much greater than the thermal skin depth. One cannot determine from a single experiment which material is the source of the radiation, but one can determine the source from examining the data of many such experiments.

Thick film shock temperatures show systematic temperature differences that depend on the film material used but not the anvil material. Figure 2 shows the results of experiments on Fe and stainless steel (SS), using both LiF and Al_2O_3 anvils. The Hugoniot temperatures for experiments on SS films are consistently higher than the ones for Fe films, as expected theoretically. There is no significant difference in the temperature achieved with different anvil materials. This result is difficult to reconcile if the radiation originates within the anvil, but it is consistent with the light originating in the metal. This is the first of several pieces of evidence supporting the transparency of Al_2O_3 during our experiments.

Thin Film Experiments

A series of shock temperature measurements was performed on thin iron films, sandwiched between two dielectric anvils. Shock temperatures are lower for dielectric anvils than for metal films. For the duration of the experiment, there is symmetric heat flow from the iron

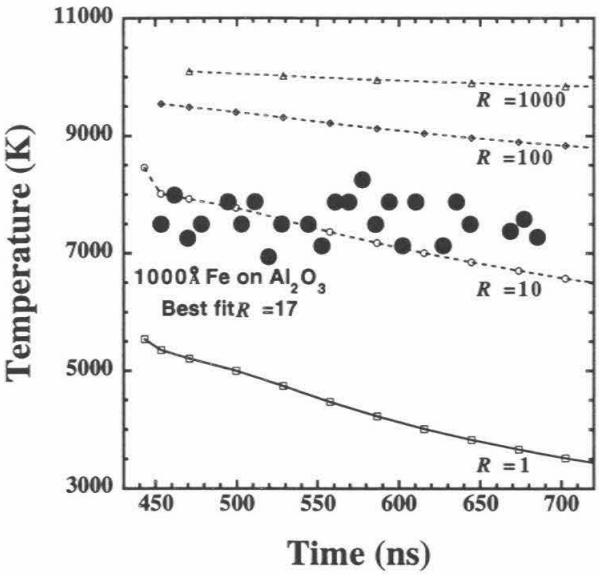

Figure 3. An experimentally observed temperature decay (Shot #287) from a 1000 Å film of Fe on an Al_2O_3 anvil at 164 GPa. The open symbols represent theoretical values for given values of R, the Fe/anvil thermal diffusivity ratio. The best fit R is 17 ± 2.

into the anvils. Because thickness is much greater than thermal skin depth, the interface temperature would not change even though heat flows across the interface [*Grover and Urtiew*, 1974]. When the film is thin, however, the interface temperature decays with time as heat flows across the boundary. We observed this decay and fit it to a finite element one-dimentional heat flow model [*King et al.*, 1989; *Gallagher and Ahrens*, 1996] to obtain thermal diffusivity ratios, R (defined by Equation 5), for the experimental materials (Figure 3). Since k_a has a $1/T$ dependence, heat conducts faster at earlier times. Thus the slope flattens out after about 40 ns of heat conduction; this correspond to times labeled 450 ns on Figure 3. Table 1 shows the best fit R values and corrects values given previously [*Gallagher and Ahrens*, 1996]. In the table, P_h is the Hugoniot pressure of the iron or of the anvil material during the experiment. T_h is the calculated Hugoniot temperature of the anvil material at the given P_h. T_i is the interface temperature measured during the experiment. ΔT is the RMS error in the grey body fit to temperature after time averaging. $k_{T,P}$ is the thermal conductivity of the anvil material; both theoretical values (Equation 4), and experimentally inferred values are listed. R is the thermal diffusivity ratio (Equation 5), and calculated values, as well as ones experimentally determined by the decay of T_i during the experiment, are listed. $\Delta k_{T,P}$ and ΔR are the RMS errors in experimentally determined $k_{T,P}$ and R values.

One of the inherent difficulties in our method of observing shock temperatures of opaque metals is the possibility that calculated conductivity values, used to calculate Hugoniot temperatures from interface temperatures via Equation 1, may be inaccurate. Our experiments provide data for R, the thermal diffusivity ratio, which is related via Equation 6 to the thermal conductivity ratio needed to calculate α (Equation 2). However it appears that the experimental values of R differ from previously calculated values by a less than factor of three for Al_2O_3 and a factor of five for LiF. The use of the 'fit' $k_{T,P}$ of Table 1 rather than values calculated via Equation 4 decreases the inferred Hugoniot temperature by about 350 K.

The thin film experiments were intended to constrain the thermal diffusivity ratio of the metal/anvil interface but can also be used to address the question of the source of the radiation. The systematics are consistent with the thick film experiments, in that no difference is observed between Hugoniot temperatures observed in experiments employing LiF and those employing Al_2O_3 anvils. Additionally, we observe a signal in which temperature decays with time, with the rate of decay depending on the thickness of the film. Thinner films (200 and 500 Å) decay faster than thicker films (1000 Å). Furthermore, since R for Fe/Al_2O_3 is lower than that of Fe/LiF, a 1000 Å film on Al_2O_3 should show a slower

Table 1. Experimental and Theoretical High Temperature and Pressure Thermal Conductivities of Corundum (Al_2O_3) and Griceite (LiF).

Shot #	Anvil	P_h (GPa) anvil	P_h (GPa) iron	T_h (K) anvil	T_i (K) interf.	ΔT_i ($\pm$K) interf.	$k_{T,P}$ ($\frac{W}{mK}$) calc.	$k_{T,P}$ ($\frac{W}{mK}$) fit	Δk ($\frac{W}{mK}$) fit	R Fe/anvil calc.	R Fe/anvil fit	ΔR ($\pm$) fit
285	Al_2O_3	244	303	2747	11000	120	16.5	6	2	70.5	19	12
286	LiF	166	261	4217	10200	490	8.57	2.3	1	29.1	11	13
287	LiF	164	269	4186	7550	520	12.6	3.4	1	11.4	4.3	11
296	Al_2O_3	165	197	1412	2×10^6	2×10^5	33.3	12	3	62.9	17	12
297	Al_2O_3	164	196	1406	6451	1030	33.4	12	3	62.7	17	13
304	Al_2O_3	156	194	1293	4813	677	35.3	13	3	58.0	16	12

decay than a film of the same thickness on LiF (Figure 4). If anvil material were the source of the observed radiation, then the decay time should not depend on film thickness.

In our thin film experiments the temperatures decay while emissivities remain approximately constant, giving an overall decrease in radiation with time. If the source of the radiation had been the anvil, then the effective observed emissivity should have increased with time because as more of the anvil material enters the shock state, more of it would be radiating. This is one of several pieces of evidence supporting the transparency of Al_2O_3 during our experiments.

Tang [1996] states that thermal contact resistance at the metal/anvil interface could be important in reducing shock temperature data. Because a contact resistance would allow a thermal boundary layer at the interface [*Swarts and Pohl*, 1989], Tang interprets the initial high intensity that is seen in some experiments as being a measure of the temperature in the interior of the metal. We disagree with this interpretation for two reasons. First, for many of our best sample assemblies we see no initial flash. If the flash was caused by an intrinsic thermal contact resistance then it would be seen in all experiments, not just some. For this reason we prefer to explain the initial intensity of some samples as being a gap flash caused by an imperfect interface. Second, if Tang's interpretation is correct, we would expect the temperature of the initial flash to be consistent from experiment to experiment, but the observed grey body temperatures of the initial rises vary over a much wider range (±800 K) than the subsequent plateau temperatures (±250 K).

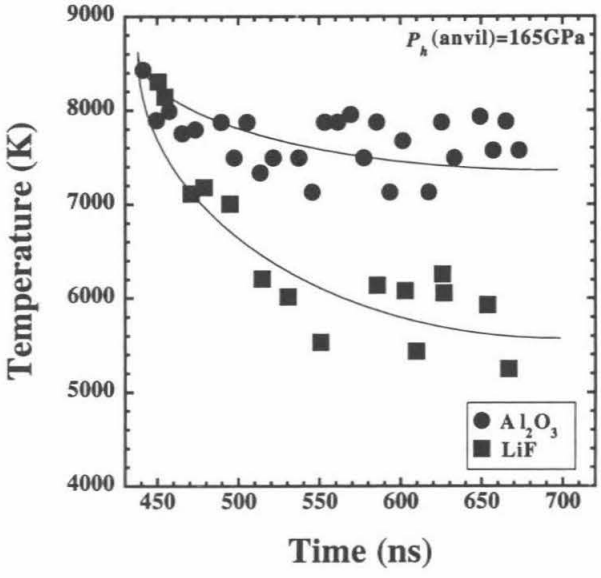

Figure 4. Comparison of conduction between Fe and (solid circles, Shot #287, P_h(Fe) = 269 GPa, P_h(LiF) = 164 GPa), and between Fe and Al_2O_3 (solid squares, Shot #297, P_h(Fe) = 196 GPa, $P_h(Al_2O_3)$ = 164 GPa). Interface temperatures decrease as heat conducts out of the 1000 Å Fe films into the anvils.

RADIATION FROM ANVIL MATERIALS

The reason the radiating anvil material is not observed is related to the large differences in T_h for the metal films and the relatively low shock temperatures of the anvils. There are two possible causes for radiation from the anvil, shear banding and grey-body emission from the continuum. If we were observing continuum anvil radiation, the amount of radiating material would increase with time (as the shock wave traverses the sample, it heats more and more of it), so the temperature would remain constant and the emissivity would increase with time. This would give an overall increase in photon flux with time. With a six channel pyrometer, we can resolve the emissivity time-dependence from the temperature time-dependence. In one experiment where the iron Hugoniot pressure was greater than 300 GPa (242 GPa in the Al_2O_3) this was observed; however, it was not the case for the other experiments, and we have never seen this behavior with LiF. Thus the radiation is not originating from the continuum of the anvil material for LiF and for Al_2O_3 below 242 GPa. If the radiation were caused by shear banding in the anvil material then, again, the amount of material involved in shear banding would increase with time, and the observed radiant intensity would increase with time. Additionally, shear banding dielectrics typically have very low emissivities $\epsilon \leq 10^{-2}$ [*Kondo and Ahrens*, 1983] whereas metals have emissivities in the range $0.1 \leq \epsilon \leq 1.0$. Our experiments show emissivities in the range 0.19 - 0.33. Therefore we conclude that for LiF and for Al_2O_3 below $\sim$ 240 GPa the radiation observed is from the iron and not the anvil. This is one of several pieces of evidence supporting the transparency of Al_2O_3 during our experiments.

As already stated, we did observe a single record that resembled *Kondo*'s [1994], where the Al_2O_3 Hugoniot pressure was $\sim$ 240 GPa. In this case, the radiation from the anvil material became brighter than the metal. Further we can distinguish between the two types of behaviors by examining the time dependence of emissivity. Kondo observes radiation from Al_2O_3 at Hugoniot pressures < 80 GPa, below our experimental range. Moreover he is observing radiation from Al_2O_3 against

a background radiation from Ag films that are 400 K hotter than those of iron at 90 GPa.

DISCUSSION

One drawback of the thin film experiments is that in order for thermal decay to be observable on the $\sim$ 200 ns time-scale of the experiment, the film must be so thin as to be comparable to the surface roughness of the optically polished anvil materials and therefore comparable in thickness to the size of the gap between the driver anvil and the metal. This causes the metal to achieve shock temperatures much higher than for thick iron films, 10,000 K as compared to 6000 K. The higher temperatures are useful in that they expedite heat flow during the experiments, but they are not useful as a shock temperature measurement. Thus, only thick film experiments can give reliable interface temperatures. Reliable Hugoniot temperatures can be calculated from 'thick film' experiments by employing the thermal diffusivity ratios measured in the 'thin film' experiments. Figure 5 shows Hugoniot temperatures for iron and also phase boundaries obtained from static experiments. Solid Hugoniot temperatures are expected to show a decrease in slope where they intersect the solid-liquid phase boundary. The slope should increase again where the phase boundary intersects the liquid Hugoniot. We refer to this behavior as an 'offset' in the slope. If there is a phase boundary that crosses our data then the 'offset' is so small as to be unobservable with shock temperature experiments employing Al_2O_3 and LiF anvils. Therefore the present data do not agree in detail with the phase boundary inferred by *Yoo et al.* [1993], who observed this expected effect at $\approx$ 250 GPa with shock temperature experiments of iron using diamond anvils.

Sound speed measurements by *Brown and McQueen* [1986] detect what they interpreted as the melting of iron under Hugoniot conditions at 243 $\pm$ 2 GPa. These measurements are accurate for determining the pressure of melting, but the melting temperatures inferred from the experiments are calculated theoretically. Interpolation of our data to 243 GPa yields a temperature of 5860 $\pm$ 390 K. This is within the error bars of Brown and McQueen's theoretical calculation, and $\sim$ 13% (740 K) less than the melting temperature reported for dynamic experiments which use diamond as the anvil material [*Yoo et al.*, 1993], and 15% (900 K) greater than the melting temperature extrapolated from static compression data [*Boehler*, 1994]. Recent further exploration at high pressures and temperatures by *Yoo et al.* [1995, 1997] suggest that our knowledge of the Fe phase diagram is incomplete.

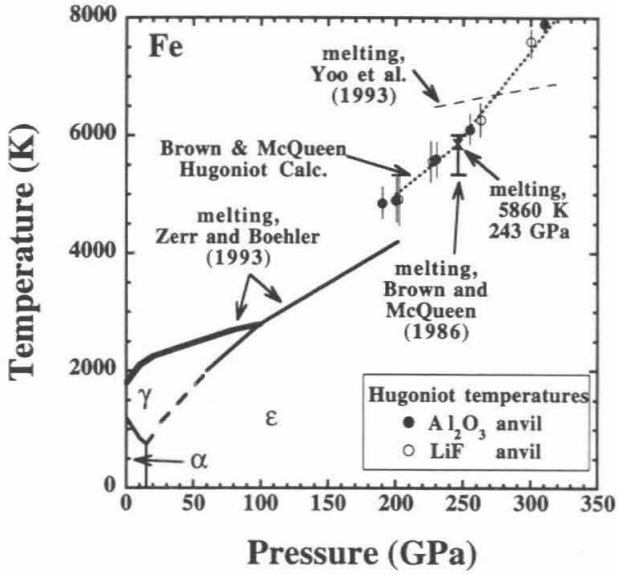

Figure 5. Hugoniot temperatures for Fe from thick film experiments using R values determined from thin film experiments. Both Al_2O_3 (solid circles) and LiF (open circles) anvils were used. Solid lines represent phase boundaries as reported by static measurements [*Boehler*, 1994]. The indicated uncertainty at 243 GPa represents melting determined via sound speed measurements [*Brown and McQueen*, 1986]. The 'X' represents our interpolated Hugoniot temperature of 5860 $\pm$ 390 K at 243 $\pm$ 2 GPa. The dotted line represents calculated Hugoniot temperatures from model b of the Brown and McQueen paper, which assumed γ = 1.34 and $\left.\frac{dE}{dP}\right|_{v_0}$ = 0.051 m^3/Mg.

CONCLUSIONS

For our experiments the anvil materials LiF and Al_2O_3 are shown to be transparent, using several lines of reasoning: First, there is a predictable systematic difference between Hugoniot temperatures of Fe and stainless steel. Second, there is no systematic dependence upon anvil material used for Hugoniot temperatures of Fe. Third, we observe a time dependence for emissivity, but no systematic time dependence for interface temperature during our 'thin film' experiments. Fourth, due to the high shock pressures of our Fe films, $P_h > 190$ GPa and due to the high temperatures caused by effective porosity in our 'thin films' experiments, our 'thin films' of Fe are expected to emit much more light than the 'thick films' of Ag reported by *Kondo* [1994] for lower pressures, < 80 GPa. Thus, light from our films

more easily overwhelms any light from the continuum thermal emission of the anvil media.

We successfully conducted 'thin film' experiments to measure R. For Al_2O_3, values of 16 to 19 were obtained, which are up to a factor of 3 lower than calculated. For LiF, values of 4.3 to 11 were obtained, which are up to a factor of 5 lower than calculated.

Experimental R values were used to revise Hugoniot temperatures on Fe. The revised shock temperatures do not show the expected offset in slope as the Hugoniot intersects the fusion curve, so neither the shock pressure of the onset of melting nor that of the completion of melting is clearly obtained. However, we report here a Hugoniot temperature of 5860 $\pm$ 390 K at the 243 $\pm$ 2 GPa, the pressure where sound speed measurements detect the onset of melting of iron.

Acknowledgments. Research supported by NSF grant EAR 92-19906 (Ahrens), EAR 95-06377 (Ahrens) and DMR 92-02587 (Atwater). We thank Neil Holmes and Michael Manga for their prompt and helpful reviews. We thank Harry Atwater and Imran Hashim for use of the argon ion sputtering apparatus and for invaluable aid in making the iron coatings used for our 'thin film' experiments. We are grateful to Raymond Jeanloz and Michael Manga for technical discussions, to Stanley Love and Jessica Faust for helpful comments on the manuscript, as well as to M. Long, E. Gelle, A. Devora and Paul Carpenter for experimental assistance. Contribution No. 5847, Division of Geological and Planetary Sciences.

REFERENCES

Ahrens, T. J., Shock wave techniques for geophsyics and planetary physics, *Meth. of Exp. Phys.*, Vol. 24, edited by C. L. Luke, pp. 185–235, Academic Press, New York, 1987.

Ahrens, T. J., J. D. Bass, and J. R. Abelson, Shock temperatures in metals, in *Shock Compression of Condensed Matter - 1989*, edited by S. C. Schmidt, J. N. Johnson, L. W. Davidson, pp. 851–857, Elsevier, Amsterdam, 1990.

Boehler, R., The phase diagram of iron to 2 Mbar: New static measurements, in *High-Pressure Science and Technology - 1993*, edited by S. C. Schmidt, J. W. Shaner, G. A. Samara, M. Ross, pp. 919–922, AIP Press, New York, 1994.

Brown, J. M., and R. G. McQueen, Phase transitions, Grüneisen parameter, and elasticity for shocked iron between 77-GPA and 400-GPa, *J. Geophys. Res., 91*, 4785–4794, 1986.

Duffy, T., and T. J. Ahrens, Thermal expansion of mantle and core materials at very high pressures, *Geophys. Res. Lett., 20*, 1103–1106, 1993.

Gallagher, K. G., J. D. Bass, T. J. Ahrens, M. Fitzner, and J. R. Abelson, Shock temperature of stainless steel and a high pressure-high temperature constraint on thermal diffusivity of Al_2O_3, in *High-Pressure Science and Technology - 1993*, edited by S. C. Schmidt, J. W. Shaner, G. A. Samara and M. Ross, pp. 963–968, AIP Press, New York, 1994.

Gallagher, K. G., and T. J. Ahrens, Ultra-high-pressure thermal-conductivity measurements of griceite and corundum, in *Shock Waves, Vol. 2*, edited by B. Sturtevant, J. E. Shepherd and H. G. Hornung, pp. 1401–1406, World Scientific, Singapore, 1996.

Grover, R., and P. A. Urtiew, Thermal relaxation at interfaces following shock compression, *J. App. Phys., 45*, 146–152, 1974.

Hashim, I., B. Park, and H. Atwater, Epitaxial growth of Cu (001) on Si (001): Mechanisms of orientation development and defect morphology, *Appl. Phys. Lett., 63*, 2833–2835, 1993.

King, S. D., A. Raefsky, and B. H. Hager, ConMan: vectorizing a finite element code for incompressible two-dimensional convection in the earth's mantle, *Phys. Earth. Plan. Int., 59*, 195–207, 1989.

Kondo, K., and T. J. Ahrens, Heterogeneous shock-induced thermal radiation in minerals, *Phys. Chem. Min., 9*, 173–181, 1983.

Kondo, K.-I., Window problem and complementary method for shock-temperature measurements of iron, in *High-Pressure Science and Technology - 1993*, edited by S. C. Schmidt, J. W. Shaner, G. A. Samara and M. Ross, pp. 1555–1558, AIP Press, New York, 1994.

Leibfried, G., and E. Schlömann, Wärmeleitung in elektrisch isolierenden kristallen. *Nachr. Akad. Wiss. Göttingen, Math Phys. Klasse I A, 4*, 71–73, 1954.

Manga, M., and R. Jeanloz, Implications of a metal-bearing chemical boundary layer in D" for mantle dynamics, *Geophys. Res. Lett., 23*, 3091–3094, 1996.

Manga, M., and R. Jeanloz, Thermal conductivity of corundum and periclase and implications for the lower mantle, *J. Geophys. Res., 102*, 2999–3008, 1997.

Matassov, G., The electrical conductivity of iron-silicon alloys at high pressures and the Earth's core, Ph.D. Thesis, University of California, Livermore, Chapter 7, 1977.

McQueen, R. G., and D. G. Isaak, Characterizing windows for shock wave radiation studies, *J. Geophys. Res., 95*, 21752–21765, 1990.

Nellis, W. J., and C. S. Yoo, Issues concerning shock temperature measurements of iron and other metals, *J. Geophys. Res., 95*, 21749–21852, 1990.

Roufosse, M. C., and R. Jeanloz, Thermal conductivity of minerals at high pressure: the effect of phase transitions, *J. Geophys. Res., 88*, 7399–7409, 1983.

Secco, R. A., and H. H. Schloessin, The electrical-resistivity of solid and liquid Fe at pressures up to 7 GPa, *J. Geophys. Res., 94*, 5887–5894, 1989.

Schmitt, D. R., B. Svendsen, and T. J. Ahrens, Shock induced radiation from minerals, in *Shock Waves in Condensed Matter*, edited by Y. M. Gupta, pp. 261–265, Plenum Publishing Corporation, New York, 1986.

Schmitt, D. R., and T. J. Ahrens, Shock temperatures in silica glass: implications for modes of shock-induced deformation, phase transformation, and melting with pressure, *J. Geophys. Res., 94*, 5851–5871, 1989.

Swartz, E. T., and R. O. Pohl, Thermal boundary resistance, *Rev. Mod. Phys, 61*, 605–668, 1989.

Tan, H., and T. J. Ahrens, Shock temperature measure-

ments for metals, *High Pressure Research, 2*, 159–182, 1990.

Tang, W., The pressure and temperature dependence of thermal conductivity for non-metal crystals, *Chinese J. High Press. Phys., 8*, 125–132, 1994.

Tang, W., F. Jing, R. Zhang, and J. Hu, Thermal relaxation phenomena across the metal/window interface and its significance to shock temperature measurements of metals, *J. Appl. Phys., 80*, 3248–3253, 1996.

Williams, Q., R. Jeanloz, J. D. Bass, B. Svendson, and T. J. Ahrens, Melting curve of iron to 250 GPa: a constraint on the temperature of the earth's center, *Science, 236*, 181–183, 1987.

Yang, W., Impact volaatilization of calcite and anhydrite and the effect on global climate from K/T impact crater at Chicxulub, Ph.D. thesis, California Institute of Technology, Chapter 4, Pasadena, CA, 1996.

Yoo, C. S., N. C. Holmes, M. Ross, D. J. Webb, and C. Pike, Shock temperatures and melting of iron at earth core conditions, *Phys. Rev. Lett., 70*, 3931–3934, 1993.

Yoo, C. S., J. Akella, A. J. Campbell, H. K. Mao, and R. J. Hemley, Phase-diagram of iron by in-situ x-ray-diffraction - implications for earth core, *Science, 270*, 1473–1475, 1995.

Yoo, C. S., A. J. Campbell, H. K. Mao, and R. J. Hemley, Detecting phases of iron - Response, *Science, 275*, 96–96, 1997.

T. J. Ahrens and K. G. Holland, Lindhurst Laboratory of Experimental Geophysics, Seismological Laboratory, California Institute of Technology, Pasadena, CA 91125. (e-mail: kathleen@gps.caltech.edu; tjacaltech.edu)